Journal of Nondestructive Evaluation, Vol. 23, No. 3, September 2004 (© 2004)

Eddy Current Assessment of Near-Surface Residual Stress in Shot-Peened Nickel-Base Superalloys

Mark P. Blodgett[1] and Peter B. Nagy[2,3]

Received February 20, 2004; revised June 15, 2004

It is shown in this paper that, in contrast with most other materials, shot-peened nickel-base superalloys exhibit an apparent increase in eddy current conductivity at increasing inspection frequencies, which can be exploited for nondestructive residual stress assessment of subsurface residual stresses. It has been found that the primary reason why nickel-base superalloys, which are often used in the most critical gas-turbine engine components, lend themselves easily for eddy current residual stress assessment lies in their favorable electro-elastic behavior, namely that the parallel stress coefficient of the eddy current conductivity has a large negative value while the normal coefficient is smaller but also negative. As a result, the average stress coefficient is also large and negative, therefore the essentially isotropic compressive plane state of stress produced by most surface treatments causes a significant increase in conductivity parallel to the surface. The exact reason for this unusual behavior is presently unknown, but the role of paramagnetic contributions cannot be excluded, therefore the measured quantity will be referred to as "apparent" eddy current conductivity. Experimental results are presented to demonstrate that the magnitude of the increase in apparent eddy current conductivity correlates well with the initial peening intensity as well as with the remnant residual stress after thermal relaxation.

KEY WORDS: Eddy current; shot peening; residual stress.

1. INTRODUCTION

Shot peening is known to improve the resistance to fatigue and foreign-object damage in metallic components due to its damage arresting qualities. This surface enhancement process, which introduces beneficial residual stresses and hardens the surface, is widely used in a number of industrial applications, including gas-turbine engines. Modern aircraft turbine engine components are designed using a damage-tolerance philosophy that allows the prediction of a given component's useful service life based on fracture mechanics and structural analysis. However, the fatigue life improvement gained via surface enhancement is not explicitly accounted for in current engine component life management processes. Therefore, there is thought to be a significant potential for increasing the predicted damage tolerance capabilities of components if beneficial residual stress considerations are incorporated into the life prediction methodology. Nondestructive inspection of components for near-surface flaws is a critical part of life assessment for many US Air Force engine applications. A major barrier to introducing subsurface residual stress information into the life calculation process is the necessity to make accurate and reliable nondestructive measurements on shot-peened hardware. In this paper, we investigate the effects of shot peening on the apparent eddy current conductivity (AECC) of several alloys, including Ti-6Al-4V and two nickel-base superalloys (Waspaloy and IN100). As a bridge to understanding

[1] Metals, Ceramics, and NDE Division, AFRL, Wright-Patterson Air Force Base, Dayton, Ohio 45433-7817.
[2] Department of Aerospace Engineering and Engineering Mechanics, University of Cincinnati, Cincinnati, Ohio 45221-0070.
[3] Corresponding author: E-mail: peter.nagy@uc.edu

Report Documentation Page

Form Approved
OMB No. 0704-0188

1. REPORT DATE	2. REPORT TYPE	3. DATES COVERED
15 JUN 2004		**00-00-2004 to 00-00-2004**

4. TITLE AND SUBTITLE	5a. CONTRACT NUMBER
Eddy Current Assessment of Near-Surface Residual Stress in Shot-Peened Nickel-Base Superalloys	5b. GRANT NUMBER
	5c. PROGRAM ELEMENT NUMBER
6. AUTHOR(S)	5d. PROJECT NUMBER
	5e. TASK NUMBER
	5f. WORK UNIT NUMBER
7. PERFORMING ORGANIZATION NAME(S) AND ADDRESS(ES) **Air Force Research Laboratory,Metals, Ceramics, and NDE Division,Wright Patterson AFB,OH,45433-7817**	8. PERFORMING ORGANIZATION REPORT NUMBER
9. SPONSORING/MONITORING AGENCY NAME(S) AND ADDRESS(ES)	10. SPONSOR/MONITOR'S ACRONYM(S)
	11. SPONSOR/MONITOR'S REPORT NUMBER(S)

12. DISTRIBUTION/AVAILABILITY STATEMENT
Approved for public release; distribution unlimited

13. SUPPLEMENTARY NOTES

14. ABSTRACT

15. SUBJECT TERMS

16. SECURITY CLASSIFICATION OF:			17. LIMITATION OF ABSTRACT	18. NUMBER OF PAGES	19a. NAME OF RESPONSIBLE PERSON
a. REPORT **unclassified**	b. ABSTRACT **unclassified**	c. THIS PAGE **unclassified**	**Same as Report (SAR)**	**17**	

the eddy current results on shot-peened specimens, we examine the effects of uniaxial mechanical loading on the AECC using both directional (elliptical) and nondirectional (circular) eddy current probes. The main result of this paper is the observation that the changes in AECC caused by shot peening and subsequent thermal relaxation are consistent with the effects resulting from uniaxial tension and compression loading. Moreover, for certain nickel-base alloys, the AECC and the compressive residual stress arising from shot peening appear to correlate uniquely, which leads us to believe the eddy current approach may provide a window of opportunity for residual stress profiling.

The goal of this research is to develop nondestructive residual stress measurement techniques for a US Air Force research initiative known as Engine Rotor Life Extension.[1,2] Under this initiative, the Air Force Research Laboratory (AFRL) has been sponsoring research to develop capabilities to, among other things, nondestructively measure subsurface residual stresses in surface-treated titanium and nickel alloys. Shot peening is the main surface treatment of interest, along with laser peening and low-plasticity burnishing, which provide a deeper zone of compression and significantly less cold work than shot peening. For gas-turbine engines, fracture-critical components are currently shot peened in the (Almen) intensity range of 3A–8A, which results in a hardened zone of near-surface compressive residual stress. The depth of compression is typically about 150–200 μm and the goal is to develop a nondestructive capability to measure the stress profile, with approximately 25 μm depth resolution, over the entire compressive zone. A critical requirement is that the measurement must be also capable of sensing small changes in the level of the remaining residual stress, since residual stresses may slowly relax over time as the component is subjected to the harsh turbine engine environment.

Currently, the only reliable NDE method for residual stress assessment is based on X-ray diffraction (XRD) measurement that is limited to an extremely thin (less than 20 μm) surface layer,[3–5] which is approximately one order of magnitude less than the typical penetration depth of compressive residual stresses produced by currently used surface treatment procedures. Recent research efforts at AFRL have shown that stress relaxation in this thin top layer occurs even at very modest temperatures and is essentially instantaneous at higher operational temperatures. Therefore, without destructive sectioning, XRD cannot provide the sought information on subsurface residual stresses for life prediction purposes. The commonly used hole-drilling method is based on measuring the change in surface strain caused by relieving the prevailing residual stress by drilling a hole in the specimen. Removing the stressed material causes a readjustment in the surrounding material to attain equilibrium, which can be quantitatively measured by strain gauges mounted in the vicinity of the hole. Unfortunately, such destructive measurement techniques are not applicable to periodic maintenance of gas-turbine engine components.

Turbine engine components are designed to optimize aircraft performance, while accommodating the adverse effects of demanding service conditions. During operation on an aircraft, many engine components are subjected to severe thermal and mechanical cycling conditions, which is presumed to cause damage and may also cause the residual stress and cold work profiles to relax over time, thereby gradually losing the protection afforded by shot peening. Some USAF engines are periodically disassembled and critical components, such as turbine disks, are subjected to intensive nondestructive inspections to ensure that dimensional tolerances are met and surfaces are free from life-limiting flaws. Many individual components are cleaned and inspected by visual, fluorescent dye-penetrant, ultrasonic, and eddy current means in an effort to detect surface-breaking fatigue cracks, fretting damage, foreign-object-damage, and other features such as dents and gouges.

Eddy current inspection is an obvious candidate for use in characterizing the residual stresses resulting from shot peening, due to its frequency-dependent penetration depth.[6–14] Unfortunately, it is well known that eddy current conductivity is affected by a number of things beside residual stress, such as chemical composition, microstructure, hardness, surface roughness, temperature, etc. Therefore, it is essential to make an assessment of the relationship of the eddy current conductivity with stress, acting alone, on the alloys of interest. The sensitivity of eddy current conductivity to stress may be easily demonstrated by putting a sample of the alloy into a load-frame and subjecting it to changing stress conditions over a fairly broad range of both compressive and tensile loads within the elastic limits. Some examples of the effect of stress on eddy current conductivity, the so-called electro-elastic effect, are provided in this paper to help illustrate why we contend that there may exist a window of opportunity for successful application of this type of eddy current-based residual stress measurement in some nickel-base superalloys. Eddy current conductivity measurements

on shot-peened engine components, both prior and subsequent to service, are currently not part of the standard inspection protocol. However, with appropriate calibration standards and tracking methods of the initial shot peening conditions and material parameters, such as microstructure and alloy composition, quantitative eddy current measurements could be made on the same critical engine components to complement routine eddy current flaw inspections.

The shot peening process involves impinging the surface with a stream of uniformly sized spherical projectiles. The plastic deformation generated by the shot impact causes an instantaneous tensile stress in the dimple and a subsequent contraction, resulting in a remnant compressive residual stress zone beneath the dimple. By overlapping the dimple coverage, a more or less homogeneous compressive residual stress zone is created over a shallow surface layer in the shot-peened region. For engine components, shot peening is controlled using specific guidelines on the shot diameter and uniformity, shot velocity, impact angle of the shot stream, and the percentage of area coverage. Shot peening plastically deforms the surface of metal components, resulting in more or less uniform but random surface roughness, a near-surface layer of compressive residual stress, and a shallow cold worked layer. Shot peening is performed on a wide range of applications, including Ti- and Ni-base gas-turbine engine components, where the resulting combination of hardening and compressive residual stress significantly improves resistance to fatigue and wear. Shot peening also serves as a surface finishing procedure performed on parts to seal-up microscopic damage and reverse tensile residual stress fields introduced by machining.

On actual engine hardware, the shot peening parameters are based on fatigue and control sample studies from identical alloys, where thermal and mechanical interactions may be examined and the use of destructive residual stress profiling techniques, such as X-ray diffraction, is feasible. However, suitable nondestructive techniques are absolutely required to successfully implement residual stress protection as a strategy for component life extension, since the actual degree of stress relaxation is especially difficult to predict because of the varying level of cold work present in surface-treated components, which exerts a profound effect on the rate of stress relaxation. Moreover, there are currently no adequate onboard engine monitoring or tracking devices to serve as a basis for predicting the degree of protection loss for shot-peened engine components due to usage.

To the best of our knowledge, no nondestructive profiling techniques are currently established that could meet the measurement needs for subsurface residual stress in terms of component life extension. The eddy current approach is attractive for this purpose because it is presently the workhorse for nondestructive inspection of military turbine engine components. Current periodic nondestructive inspections of engine components revolve around the detection of near-surface flaws and often involve differential eddy current techniques to optimize the probability of detection, rather than to map the eddy current conductivity. Eddy current based characterization of residual stress is also very attractive from the standpoint of available instrumentation, since state-of-the-art eddy current instruments enjoy the benefits of several decades of development. Currently, there is already a substantial eddy current inspection infrastructure geared for flaw detection in place, which could be easily branched over to residual stress characterization via AECC spectroscopy. However, the apparent eddy current conductivity is obviously influenced by a number of different variables such as surface roughness, microstructure, magnetic permeability, etc. Therefore, great care must be taken in its measurement and interpretation and further research is needed to determine if the approach can be made into a practical, quantitative means of assessing subsurface residual stresses for life prediction purposes.

Most turbine engine components of interest are comprised of either titanium alloys or nickel-base superalloys, which all have strict requirements on impurity tolerances, heat treatments, and microstructure characteristics to qualify as rotor-grade material. For titanium alloys, the material generally solidifies in a hexagonally symmetric lattice structure for the alpha phase, which typically constitutes about 95% of the alloy volume. The processing of titanium alloys typically results in the presence of bulk crystallographic texture due to limited availability of slip systems and often there are macroscopic colonies of grains with similar crystallographic orientation. The alpha phase in titanium alloys gives rise to local variations in the AECC due mainly to the presence of these domains of crystallographic similarity, which typically affect the AECC to a larger extent than any effect due to stress. AECC variations as large as $\pm 3\%$ can be often observed in forged Ti-6Al-4V. Additionally, for Ti alloys, the surface roughness, cold work, and near surface compressive residual stress arising from shot peening all cause similar decrease in the

AECC as a function of frequency. Therefore, there exists a uniqueness problem that prevents the eddy current conductivity approach from being used for residual stress measurement in titanium alloys. Nevertheless, AECC mapping may prove to be a valuable tool to track other material properties, which evolve over time due to thermal and mechanical exposure. In contrast, the AECC of alloys solidifying in cubic symmetry, such as Ni-base superalloys, is not significantly affected by processing related material inhomogeneity, such as crystallographic texture. The refined grain structure and relatively even phase distribution of the microstructure essentially eliminates these characteristics as factors in the AECC signal since these variations are spatially averaged over the probe dimensions, which are typically 2–3 mm or larger in diameter. Most importantly, there appears to be a unique relationship between the subsurface residual stresses in certain nickel-base superalloys and variations in AECC, which is the main focus of this paper.

2. PRELIMINARY XRD AND EDDY CURRENT MEASUREMENTS

The main technical challenges to developing nondestructive techniques for characterization of subsurface residual stresses are twofold: (i) achieving the high measurement sensitivity and accuracy required for modest shot peening intensities (between Almen 3A and 8A) typically applied to engine components, and (ii) separating the primary residual stress contribution from competing secondary factors in the measurement due to texture, hardness, microstructure, surface roughness, etc. As a first step towards meeting these challenges, several Ti-6Al-4V, Waspaloy, and IN100 sample sets of Almen intensities between 4A and 16A were shot peened and tested by eddy current inspection. To get the necessary information on the subsurface residual stresses, one set of samples of each alloy was sacrificed for XRD stress measurements, using the destructive layer removal method. Figure 1 shows the residual stress profiles in shot-peened samples of three different engine alloys. These results illustrate that the shot peening intensity has a strong effect on the depth of the compressive zone, but much less on the peak value of the compressive residual stress. Furthermore, the residual stress measurements all tend to cluster on the surface, indicating one of the main reasons why surface only XRD measurements are probably insufficient for life prediction purposes.

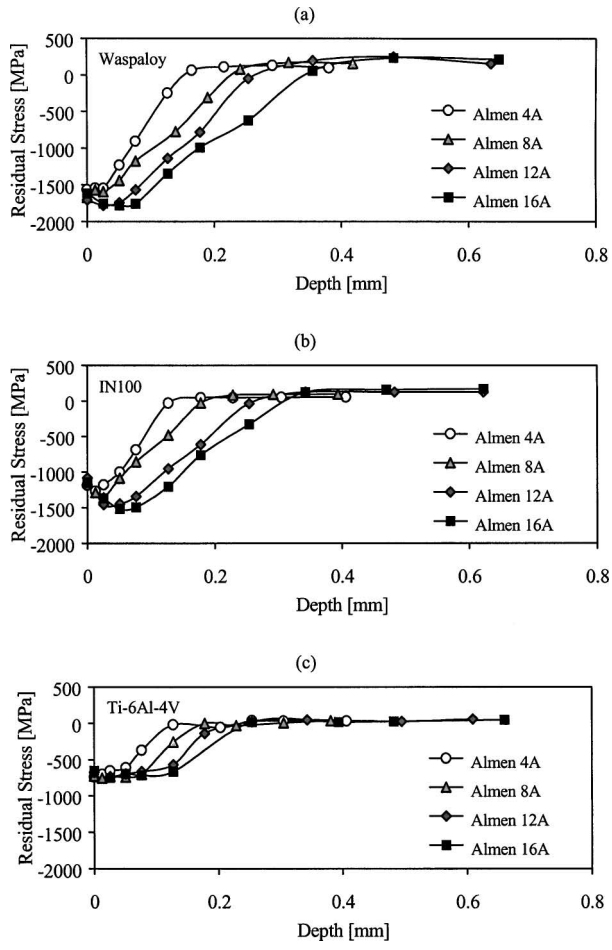

Fig. 1. Residual stress profiles in shot-peened samples of three different engine alloys.

Existing scientific evidence indicates that even when the eddy current measurements are conducted with sufficient precision the obtained parameters are affected by not only the existing residual stress profile, but also by the accompanying cold work[13] and surface roughness effects.[12,15,16] The penetration depth of the cold worked region is typically one third of that of the compressive residual stress, therefore, just like the surface roughness effect, cold work effects cannot be eliminated simply by an appropriate selection of the inspection frequency. Generally, cold work exhibits itself through lattice imperfections, such as increased dislocation density, and localized anisotropy caused by crystallographic and morphological texture. Separation of the residual stress and cold work effects requires careful optimization of the inspection method on a case-to-case basis. For example, crystallographic anisotropy strongly affects ultrasonic

surface acoustic wave (SAW) measurements in all metals except those of very low elastic anisotropy like tungsten or aluminum, but has no effect on eddy current and thermoelectric measurements in metals that crystallize in cubic symmetry, a broad category that includes essentially all engine materials with the notable exception of titanium alloys.[17,18]

It should be emphasized that for the purposes of practical nondestructive assessment of thermo-mechanical relaxation in surface-treated metals, the separation of residual stress and cold work effects is less crucial than the elimination of surface roughness effects. The main reason for this is that in most cases the decay of the subsurface residual stress is more or less proportional to the parallel decay of cold work, therefore their relative contribution to the nondestructively measured parameter is more or less constant. In comparison, the adverse effect of surface roughness is unaffected by thermo-mechanical relaxation, and might even increase as a result of additional roughening due to fretting, corrosion, or erosion, therefore its role is gradually increasing with respect to the weakening residual stress.

The characteristic dependence of electrical conductivity on stress has been thought to be very promising for residual stress measurements in metals for a long time, though these expectations have remained largely unfulfilled as far as surface-treated components are concerned. In most metals the stress-dependence of the electrical conductivity is rather weak and the primary residual stress effect is rather difficult to separate from the secondary cold work effect and, especially in shot-peened specimens, from the apparent loss of conductivity caused by the spurious surface roughness effect. In paramagnetic materials the electrical conductivity typically increases by approximately 1% under a maximum biaxial compressive stress equal to the yield strength of the material. However, the electrical conductivity measured on shot-peened specimens typically decreases with increasing peening intensity, often as much as 1–2%, which indicates that surface roughness and cold work effects dominate the observed phenomenon. We have found that, in sharp contrast with most other materials, shot-peened Waspaloy and IN100 specimens exhibit an apparent increase in electrical conductivity at increasing inspection frequencies. This observation by itself seems to indicate that in these materials the measured conductivity change is probably dominated by residual stress effects, since surface roughness, increased dislocation density, and increased permeability are known to decrease rather than increase the

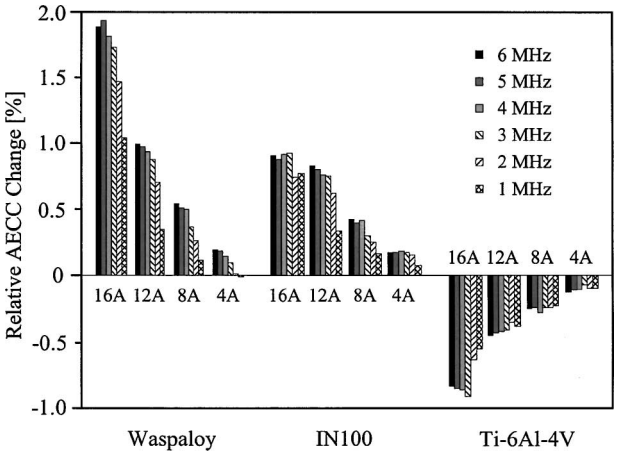

Fig. 2. Relative change in apparent eddy current conductivity (AECC) between the shot-peened sample and the unpeened equivalent for three different engine alloys over a frequency range of 1 to 6 MHz.

apparent conductivity and the presence of crystallographic texture does not affect the electrical conductivity of these materials, which crystallize in cubic symmetry.

Preliminary eddy current conductivity measurements were conducted on the remaining alloy sample sets using a Nortec 19e^{II} instrument and a 4-MHz Uniwest absolute pencil probe to observe the change in AECC due to shot peening. Figure 2 shows some of these results over a range of frequencies from 1 to 6 MHz. Of course the intrinsic electrical conductivity of the material is independent of frequency over this range. The observed frequency dependence of the eddy current conductivity is due to the depth-dependence of the electrical conductivity and the frequency dependence of the eddy current penetration depth. The apparent eddy current conductivity is calculated from the actually measured complex electrical impedance of the probe coil by assuming a perfectly flat and smooth homogeneous conducting half-space of zero magnetic susceptibility, therefore could be also significantly affected by variations in magnetic material properties (permeability) as well as spurious geometrical effects (surface roughness). In order to indicate the potential influence of these uncorrected effects on the measured quantity, we will call it "apparent" eddy current conductivity or AECC.

The eddy current measurements shown in Fig. 2 are based on the difference in the AECC between the shot-peened alloy and the unpeened equivalent alloy. The measurements were calibrated using two different conductivity standards (1.03% IACS and 1.45%

IACS) in order to get the results in terms of percent change in AECC. The results of Fig. 2 demonstrate that the AECC is affected by the Almen intensity and the inspection frequency, although the influence of the inspection frequency is much clearer in the nickel-base superalloys than in the case of Ti-6Al-4V. It should be mentioned that in these preliminary measurements we used a rudimentary method to maintain lift-off consistency from sample to sample, which is especially problematic for measurements at higher frequencies, and the data acquisition approach in general was rather crude. These measurements were subsequently repeated in Waspaloy using a four-point linear interpolation approach, which better elucidated the effect of frequency, over a larger frequency range as shown in Section 4.

Based on these preliminary results, the most pronounced change in AECC occurs at the highest peening intensities, where the compressive layer is the deepest, and at the highest inspection frequencies, where the penetration depth is the smallest. The alloys tested in this study are all relatively poor conductors, with Ti-6Al-4V at approximately 1% IACS and Waspaloy and IN100 both at approximately 1.5% IACS. Hence, despite the high inspection frequencies, the standard penetration depth, which is inversely proportional to the square root of the frequency-conductivity product, is relatively large for these alloys (e.g., approximately 200 μm at 6 MHz for Waspaloy). The most important detail apparent from Fig. 2 is that the two nickel-base superalloys demonstrate a frequency-dependent increase in the AECC over the shot-peened region, while Ti-6Al-4V shows the opposite effect, which behaves like aluminum alloys and other structural materials previously studied in the literature.[6–14] This observation suggests that the residual stress is most likely responsible for the observed increase in the AECC in shot-peened nickel-base superalloy samples because the other main effects of shot peening (i.e., increased dislocation density and surface roughness) are known to cause the apparent eddy current conductivity to decrease.

There is some concern that this phenomenon could be somehow related to subtle ferromagnetic effects caused by strong elastic and plastic strains in these otherwise paramagnetic engine materials of high iron and nickel content. However, we should mention that a thin ferromagnetic surface region would cause an apparent decrease rather than increase in the measured eddy current conductivity, therefore it is unlikely to play a dominant role in the observed phenomenon. The possible influence of magnetic and microstructural variations in the cold-worked near-surface layer of shot-peened nickel-base superalloys will be separately investigated in order to better understand this phenomenon and to help develop the eddy current technique as a viable approach for subsurface residual stress characterization.

3. ELECTRO-ELASTIC EFFECT

In direct analogy to the well-known acousto-elastic effect, a widely used NDE terminology for the dependence of the acoustic velocity on elastic stress, we are going to refer to the stress dependence of the electrical conductivity as the electro-elastic effect, which is often called in the literature as the piezoresistive effect. In the presence of elastic stress $[\tau]$ the electrical conductivity tensor $[\sigma]$ of an otherwise isotropic conductor becomes slightly anisotropic. In principal coordinates,

$$\begin{bmatrix} \sigma_1 \\ \sigma_2 \\ \sigma_3 \end{bmatrix} = \begin{bmatrix} \sigma_0 & 0 & 0 \\ 0 & \sigma_0 & 0 \\ 0 & 0 & \sigma_0 \end{bmatrix} + \begin{bmatrix} K_\parallel & K_\perp & K_\perp \\ K_\perp & K_\parallel & K_\perp \\ K_\perp & K_\perp & K_\parallel \end{bmatrix} \begin{bmatrix} \tau_1 \\ \tau_2 \\ \tau_3 \end{bmatrix}, \tag{1}$$

where σ_0 denotes the electrical conductivity in the absence of stress and $K_\parallel$ and $K_\perp$ are the so-called parallel and normal electro-elastic coefficients, respectively.

The simplest example of the electro-elastic effect is exhibited by ordinary strain gauges. Under uniaxial stress ($\tau_1 = \tau$ and $\tau_2 = \tau_3 = 0$), the so-called gauge factor γ is defined as the ratio of the relative resistance change $\delta R/R_0$ and the axial strain $\varepsilon = \tau/E$

$$\gamma = \frac{1}{\varepsilon}\frac{\delta R}{R_0} \approx (1 + 2\nu) - \frac{1}{\varepsilon}\frac{\delta\sigma}{\sigma_0} = (1 + 2\nu) - K_\parallel \frac{E}{\sigma_0}, \tag{2}$$

where $\delta\sigma$ is the change in electrical conductivity and ν and E denote Poisson's ratio and Young's modulus. It is well known that the gauge factor is usually significantly higher than the first term $1 + 2\,\nu \approx 1.6$ of purely geometrical origin, which indicates that $K_\parallel$ is negative. Of course, if the average electrical conductivity $\sigma_\circ$ is measured under uniaxial stress by a unidirectional circular eddy current probe, the effective electro-elastic coefficient $K_\circ$ will be equal to the algebraic average of the parallel and normal electro-elastic coefficients, i.e.,

$$\frac{\delta\sigma_\circ}{\tau_1} = K_\circ = \frac{1}{2}(K_\parallel + K_\perp). \tag{3}$$

Another example of the electro-elastic effect in conducting metals is the pressure dependence of the electrical conductivity under hydrostatic pressure ($\tau_1 = \tau_2 = \tau_3 = -p$), when

$$\frac{\delta\sigma}{p} = -(K_{\parallel} + 2K_{\perp}). \tag{4}$$

It is well known after the classic work of Bridgman that the pressure coefficient of the electrical conductivity is negative in most structural metals, although some exceptions do occur.[19] For our immediate purposes, the most important case is that of isotropic plane stress ($\tau_1 = \tau_2 = \tau$ and $\tau_3 = 0$), when the change in the measured average conductivity in the plane of stress can be written as follows

$$\frac{\delta\sigma_{\circ}}{\tau} = 2K_{\circ} = K_{\parallel} + K_{\perp}. \tag{5}$$

Unfortunately, there is not much known in the scientific literature about the electro-elastic coefficients of high-temperature engine alloys, therefore we had to conduct a series of electro-elastic measurements to verify our working hypothesis that the increased apparent eddy current conductivity observed in shot-peened nickel-base superalloy specimens could indeed be caused by the presence of compressive near-surface residual stresses. For this purpose we prepared a series of samples to be tested in a load-frame, where the effects of stress could be singled-out versus the other shot peening effects. Figure 3 shows a schematic diagram of the experimental arrangement used to measure the electro-elastic coefficients of different engine alloys in uniaxial compression and tension. Both non-directional circular and directional racetrack coil probes were used for the load frame testing. The racetrack coils were used in directions both parallel and normal to the loading direction to observe the directional

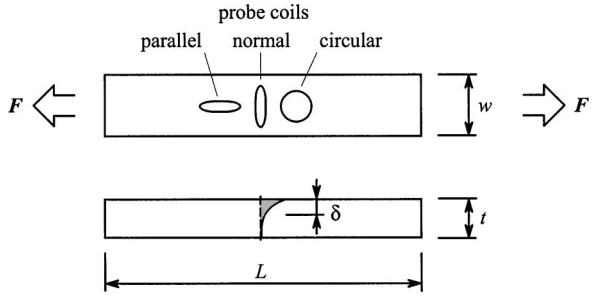

Fig. 3. A schematic diagram of the experimental arrangement used to measure electro-elastic coefficients in uniaxial compression and tension.

dependence of stress on the apparent eddy current conductivity.

Figure 4 shows examples of the axial stress and the corresponding eddy current conductivity at parallel orientation in IN718 as functions of time. Alternating axial load was applied to the specimens at a cyclic frequency of 0.5 Hz. Although we are mainly interested in the effect of compressive stresses on the electrical conductivity of the specimens, the maximum tensile load was chosen to be twice as high as the maximum compressive load in order to minimize the possibility of buckling in the slender rectangular bars used as specimens ($w = 12.5$ mm, $t = 6.35$ mm, $L \approx 150$ mm). Unless explicitly noted otherwise, these measurements were all made at $f = 300$ kHz, where the standard penetration depth ($\delta \approx 1$ mm) was much smaller than the thickness of the specimens, therefore the spurious thickness modulation caused by the Poisson effect could be neglected. These measurements were conducted over a sustained period of approximately 2 minutes so that the adverse effects of random noise and thermal drift could be sufficiently reduced via averaging. However, it is clear even from the somewhat noisy raw data shown in Fig. 4 that the parallel electro-elastic coefficient of IN718 is negative, that is the conductivity increases in compression.

Figures 5, 6, and 7 show eddy current conductivity versus stress results for Ti-6Al-4V, IN718, and Waspaloy, respectively, at both parallel and normal orientations. The symbols represent experimental data while the solid lines are best fitting linear regressions. It is apparent from these results that the behavior of parallel eddy current conductivity is quite different between Ti-6Al-4V and the two nickel-base superalloys. In the case of Ti-6Al-4V, under compressive loading the AECC in the load direction (parallel orientation) progressively decreases, while for IN718 and Waspaloy, under similar loading conditions, the AECC progressively increases. As we mentioned above in connection with Eq. (5), the effective electro-elastic constant under isotropic plane state of stress is the sum of the parallel and normal electro-elastic coefficients, $K_{\parallel} + K_{\perp}$. Therefore, it is very important that in nickel-base superalloys both coefficients are negative so that they act together to provide a relatively large increase in the apparent eddy current conductivity in shot-peened specimens.

Figure 8 demonstrates for ten repeated measurements each how the difference in signs of the parallel and normal stress coefficients results in a destructive effect on the average stress coefficient value in the case of Ti-6Al-4V (a) versus IN718 (b) where the

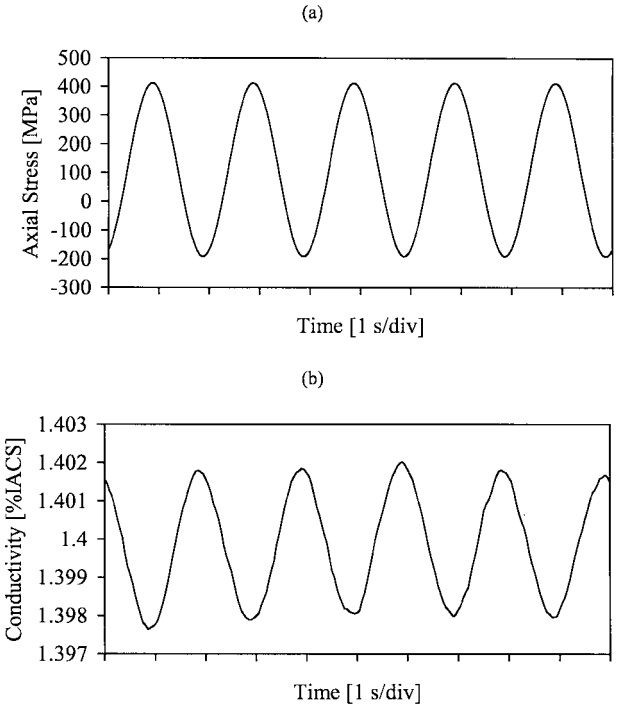

Fig. 4. An example of (a) the axial stress and (b) the eddy current conductivity at parallel orientation as functions of time in IN718.

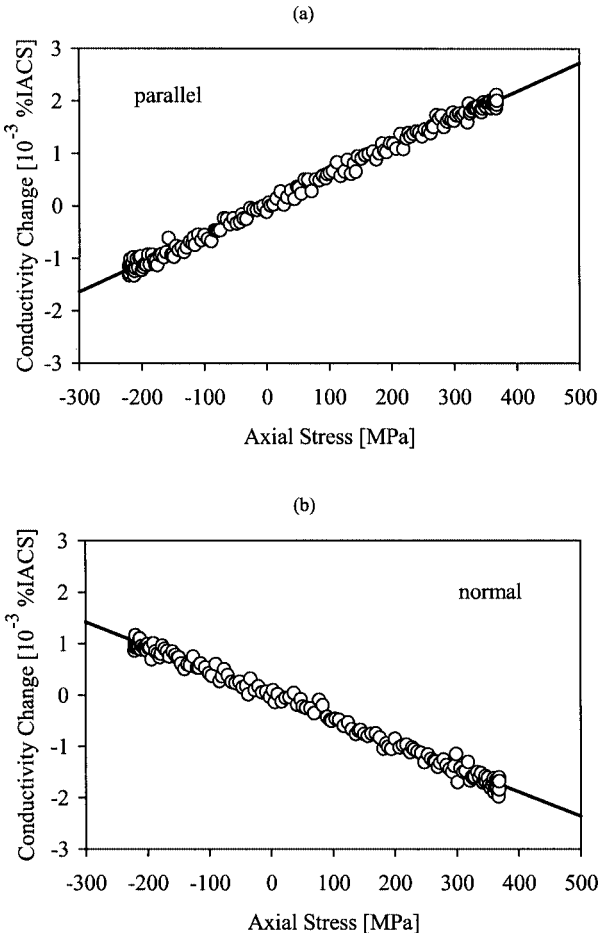

Fig. 5. Electro-elastic measurements in Ti-6Al-4V using a directional eddy current probe (a) parallel and (b) normal to the applied uniaxial load.

likeness in signs of the stress coefficients leads to a constructive effect on the average value. These results demonstrate that the anticipated role of stress in AECC measurements of shot-peened samples is expected to be marginal in the case of Ti-6Al-4V, but quite significant if not dominant, for the case of IN718.

In nickel-base superalloys there is a possibility that a thin ferromagnetic surface layer forms due to mechanical, microstructural, or chemical effects. For example, we found that the commercial quality Waspaloy used in some of our experiments, which was surface-treated by pickling (a type of chemical etching to remove the top layer), did exhibit an approximately 0.1-mm-deep ferromagnetic surface layer in the as-received state before machining and shot peening. Chemical analysis revealed that this layer was significantly depleted of Ni, Mo, and Co and rich in Cr, C, and Fe. Measurements conducted on these specimens before removing the spurious ferromagnetic surface layer by grinding showed more than one order of magnitude increase in the electro-elastic coefficients, which also showed strong signs of nonlinearity, hysteretic behavior, and frequency dependence. In order to verify that the measured electro-elastic effects in nickel-base superalloys were not significantly affected by the presence of such spurious ferromagnetic surface layers, we measured the electro-elastic coefficients in low-stress ground specimens over a wide frequency range. As an example, Fig. 9 shows the parallel and normal electro-elastic coefficients measured in engine quality Waspaloy between 100 and 800 kHz. Within the experimental uncertainty of the measurement, both electro-elastic coefficients are frequency independent, which clearly indicates that the results are not affected significantly by spurious surface effects.

The fundamental reason for the difference in electro-elastic behavior between nickel-base superalloys and Ti-6Al-4V is currently unknown, but of the large number of different materials we have tested to date, the former case appears to be the exception, rather than the rule, which is probably

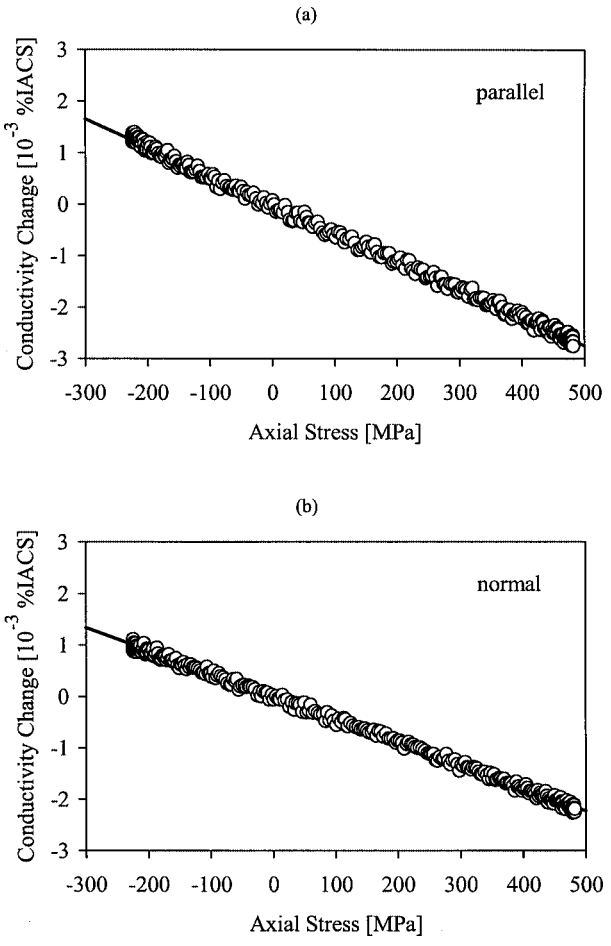

Fig. 6. Electro-elastic measurements in IN718 using a directional eddy current probe (a) parallel and (b) normal to the applied uniaxial load.

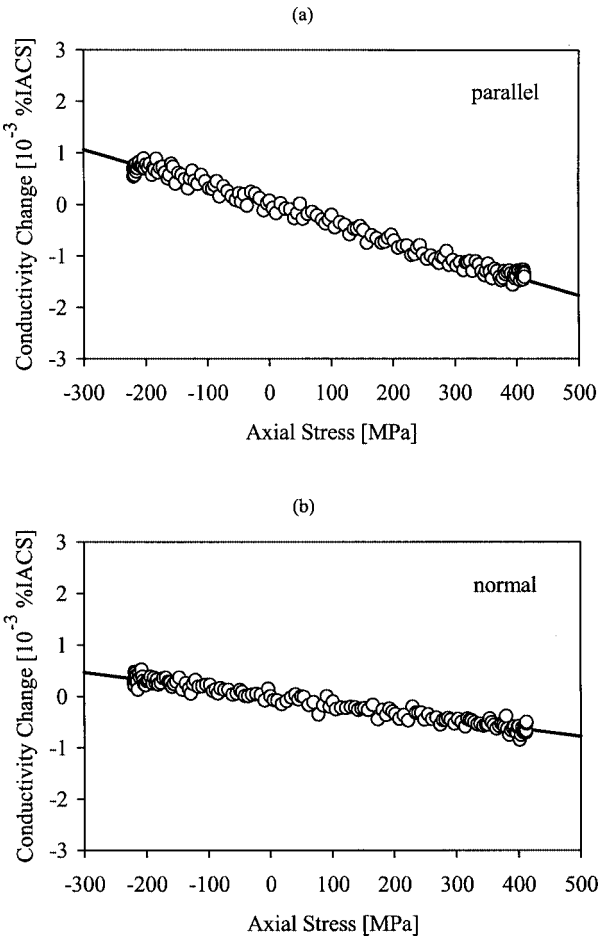

Fig. 7. Electro-elastic measurements in commercial Waspaloy using a directional eddy current probe (a) parallel and (b) normal to the applied uniaxial load.

why eddy current-based evaluation of residual stress has not been successfully demonstrated before for shot-peened specimens. Fortunately, the small group of structural metals that exhibit this beneficial electro-elastic behavior appears to include some of the most critical nickel-base superalloy materials for gas-turbine engine components, including Waspaloy, IN100, IN718, and likely many others. Table I lists the electro-elastic coefficients of various high-temperature alloys tested to date. Clearly, the three critical precipitation hardened gasturbine engine alloys (Waspaloy, IN100 and IN718) all demonstrate the potential window of opportunity for residual stress assessment by eddy current means due to their relatively large negative average electro-elastic coefficients.

Table II lists the relevant electro-elastic, electrical, and mechanical properties of high-temperature alloys, which are useful as a basis for assessing the consistency between the electroelastic effect and the AECC change observed in shot-peened specimens. The maximum expected relative change in the apparent eddy current conductivity can be estimated from

$$S = -\frac{2K_{\circ}\tau_{\max}}{\sigma_0} \tag{6}$$

where $K_{\circ}$ is the non-directional average electro-elastic coefficient, σ_0 is the unstressed electrical conductivity, and $\tau_{\max}$ is the maximum compressive residual stress due to shot peening, which is estimated from the nominal yield strength of the material. In nickel-base superalloys, the maximum relative conductivity change is predicted to be on the order of 0.5–1%, which is reasonably close to the maximum AECC increase observed in shot-peened specimens. However, there are some minor discrepancies in the

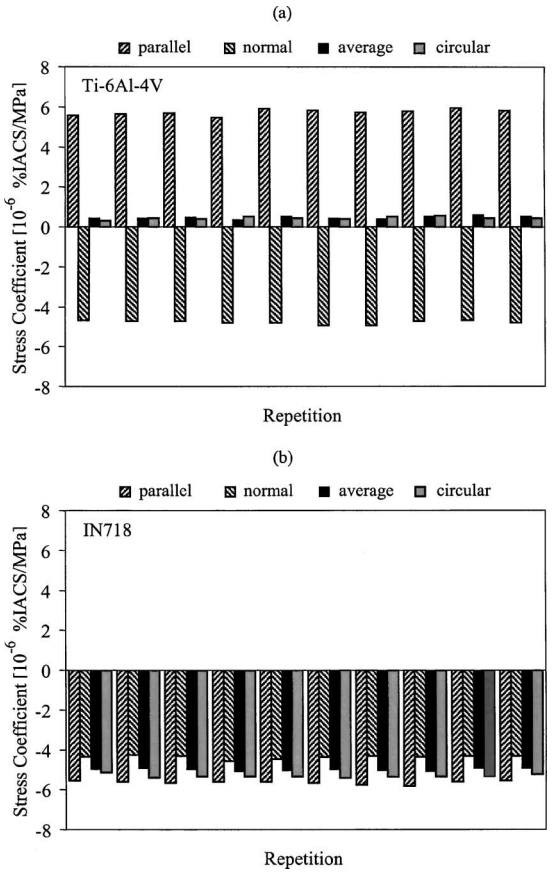

Fig. 8. A comparison the electro-elastic stress coefficients of (a) Ti-6Al-4V and (b) IN718.

results, requiring further research to better understand the physics of this approach in order to reliably and accurately characterize shot peening relaxation in turbine engine materials. Specifically, for the case of Waspaloy we would anticipate only a 0.5–0.6% change in the electrical conductivity due to stress, but in a 16A shot peened Waspaloy sample we actually measured approximately 1.8% increase at 10 MHz, relative to the unpeened equivalent alloy. The discrepancy is not so apparent for the case of the 8A shot-peened Waspaloy, where we measure only about a 1.2% change at 10 MHz, but there is still about a factor of 2 difference in terms of the anticipated change due to stress. There could be a number of reasons for this, e.g., the known fact that the presence of microstructural defects significantly increases the stress dependence of conductors,[20,21] which will be separately investigated in a follow-up project. Despite the small discrepancy for Waspaloy, we show later in this paper that the agreement between the eddy current results for characterizing shot peening stress relaxation is quite good as judged by the established XRD layer removal stress measurement technique. On the other hand, IN100 and IN718 appear to be excellent candidates for this kind of nondestructive stress measurement approach considering the nearly exact agreement between the anticipated effect of stress on conductivity and the actually measured effect in shot peened specimens.

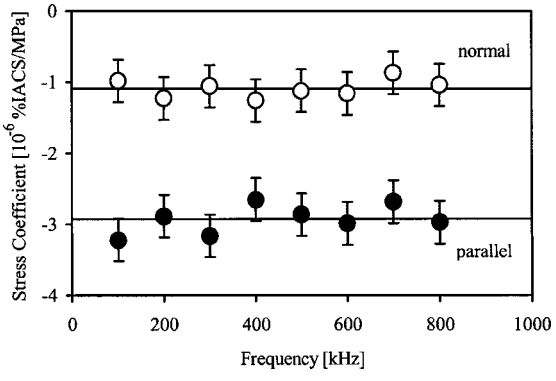

Fig. 9. Parallel and normal electro-elastic coefficients measured in engine quality Waspaloy over a wide frequency range.

Table I. Combined Results of Stress Coefficient Measurements in High-Temperature Alloys (the Average and Standard Deviation Values Are Given in 10^{-6}% IACS/MPa)

Alloy	$K_\parallel$	$K_\perp$	$1/2\,(K_\parallel + K_\perp)$	$K_\circ$
Ti-6Al-4V	+5.73/0.15	−4.79/0.09	+0.46/0.07	+0.45/0.09
Hastelloy X	−0.62/0.06	+2.97/0.22	+1.17/0.09	+1.42/0.10
IN718	−5.64/0.09	−4.38/0.09	−5.02/0.06	−5.31/0.07
IN100	−6.90/0.16	−2.09/0.23	−4.50/0.09	−5.32/0.29
Commercial Waspaloy	−3.39/0.19	−1.54/0.12	−2.47/0.10	−2.63/0.15
Engine Waspaloy	−2.93/0.10	−1.10/0.10	−2.02/0.07	−2.28/0.15

Table II. Electro-Elastic, Electrical, and Mechanical Properties of High-Temperature Alloys, Which Are Useful as a Basis for Assessing the Consistency Between the Electro-Elastic Effect and the AECC Change Observed in Shot-Peened Specimens

Alloy	$K_\circ$ [10^{-6}% IACS/MPa]	σ_0 [%IACS]	τ_{max} [MPa]	S [%]
Ti-6Al-4V	+0.45	1	680	−0.07
Hastelloy X	+1.42	1.6	410	−0.08
IN718	−5.31	1.4	1370	+1.03
IN100	−5.32	1.3	1370	+1.12
Commercial Waspaloy	−2.63	1.5	1720	+0.60
Engine Waspaloy	−2.28	1.5	1720	+0.52

In summary, more research is essential to further understand this phenomenon, including the possible role of slight permeability changes due to marginal ferromagnetism and shot peening induced microstructural effects, but the demonstrated consistency between shot peening and load-frame testing in these preliminary results appears to reinforce our position that retained stress is probably the main factor responsible for the increase in frequency-dependent AECC for shot-peened nickel-base superalloys.

4. ABSOLUTE VERSUS RELATIVE AECC MEASUREMENTS

Since our specimens were shot-peened only over half of their surface, the unpeened half could be readily used for comparison purposes. Scanning the specimens parallel to their surface allowed us to directly determine the AECC difference between the peened and unpeened parts at each inspection frequency. We are going to refer to this technique as relative measurement. The surface of the specimen is first aligned with the scanning plane of a motorized $x - y$ table, the probe is adjusted to a constant nominal lift-off distance (typically $\ell = 0.1$ mm), then the complex impedance plane is rotated by changing the phase angle so that the lift-off direction appears horizontal, and the vertical component of the impedance variation is used to assess the AECC. The adverse effects of inevitable lift-off variations during scanning are effectively reduced by this choice of the phase angle. The relative sensitivity of the system is determined at each inspection frequency using similar measurements on a pair of appropriately chosen calibration blocks. Because of its automatic scanning capability, this technique allow us to quickly inspect relatively large areas and obtain either two-dimensional AECC images of the surface or simply calculate the average difference between the peened and unpeened parts.

In spite of its obvious advantages, relative measurements of the AECC based on direct comparison of peened and unpeened parts is not practical in real applications when usually there is not such reference surface available. Instead, we have to measure the absolute AECC of the specimen as a function of frequency and compare the near-surface properties measured at high frequencies to those at larger depth measured at low-frequencies. In order to clearly distinguish this technique from the above described relative measurement, we are going to refer to it as absolute measurement.

First, additional AECC measurements were conducted on intact shot-peened Waspaloy samples in order to verify whether point-by-point absolute measurements using manual scanning or large-area relative measurements using automated scanning are better suited for the subsequent inspection of thermally relaxed specimens. These measurements were made by a Staveley Nortec 2000S eddy current instrument with three different probes to assure optimal sensitivity over a wide frequency range from 100 kHz to 10 MHz. The four-point calibration procedure used in absolute measurements is slightly more complicated than the two-point calibration used in our preliminary measurements. Figure 10 shows a schematic representation of the coil impedance in the complex plane before (a) and after (b) zoom-in and roation. For a given set of gains and phase rotation, the real $x = x(\sigma, \ell)$ and imaginary $y = y(\sigma, \ell)$ components of the measured impedance are determined by the conductivity of the specimen σ and the lift-off distance ℓ. First, the four reference points are measured on two appropriate calibration blocks with ($\ell = s$) and without ($\ell = 0$) a polymer foil of thickness s between the probe coil and the specimens.

As we discussed before, complications such as inhomogeneity, permeability effects, surface roughness, etc., are neglected during inversion of the coil impedance, therefore the measured frequency-dependent quantity is referred to as apparent eddy current conductivity or AECC. The coil impedance measured on the shot-peened specimens is evaluated in terms of apparent conductivity and lift-off using simple linear interpolation (though the lift-off data was subsequently discarded). It should be mentioned that the linear interpolation technique, which is known to leave much to be desired over larger

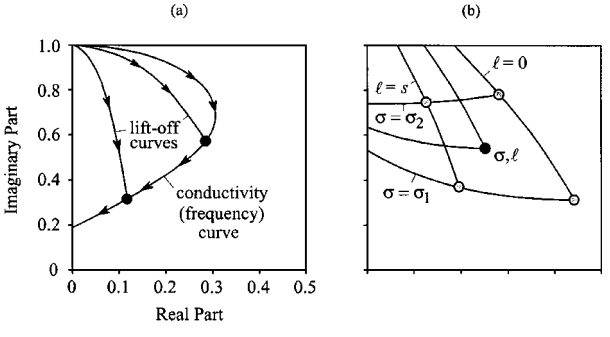

Fig. 10. A schematic representation of the coil impedance in the complex plane before (a) and after (b) zoom-in and rotation demonstrating the four-point linear interpolation procedure for acquisition of the AECC data.

measurement ranges, was quite sufficient over the relatively small conductivity range considered in this study. Because of the high precision requirements of these measurements, efficient rejection of inevitable lift-off variations is of the utmost importance. It was also necessary to periodically repeat the calibration procedure during manual scanning in order to reduce the adverse effects of thermal drift caused by the weak, but still perceivable instability of the probe and the instrument. The statistical variations over the 50.8 mm × 50.8 mm shot-peened areas were kept under control by repeating all measurements at 50 different locations and averaging the data for each frequency, which also reduced the incoherent scatter in the data caused by thermal oscillations, electrical noise, imperfect lift-off rejection, etc. With such measures, the accuracy of the averaged data is expected to be better than ±0.002% IACS, i.e., approximately ±0.15% relative to the 1.5% IACS baseline conductivity of nickel-base superalloys.

For the following absolute measurements the experimental system was calibrated at each inspection frequency using two standardized reference blocks of $\sigma_1 = 1.34\%$ IACS and $\sigma_2 = 1.48\%$ IACS and an $s = 0.076$-mm-thick polymer foil for controlling lift-off (above 4 MHz the thickness of the polymer foil was reduced to 0.025 mm). Figures 11a and 11b show the results of the eddy current measurements on the smooth untreated and the shot-peened surfaces, respectively, for each of the four different peening intensities over a range of 100 kHz to 10 MHz. These results were collected using manual scanning taking 50 randomly located individual measurements (away from the edges) at each frequency from both the untreated and shot-peened surfaces and averaging the data. The measurements from the untreated surfaces show only a very mild decrease in AECC with increasing frequency, while the shot peened surfaces exhibit an increasing AECC as a function of frequency for each peening intensity.

Figure 12 shows the difference between the untreated and shot-peened surfaces for each peening intensity using two different methods. Figure 12a shows the difference between the corresponding absolute measurements obtained by manual testing, which were previously shown in Fig. 11. Figure 12b shows the results of the relative AECC measurements obtained by computer-controlled automatic scanning. A comparison between these results reveals a minor discrepancy in the magnitudes of the AECC differences between the manual versus automated testing approaches. At this point, the exact reason for

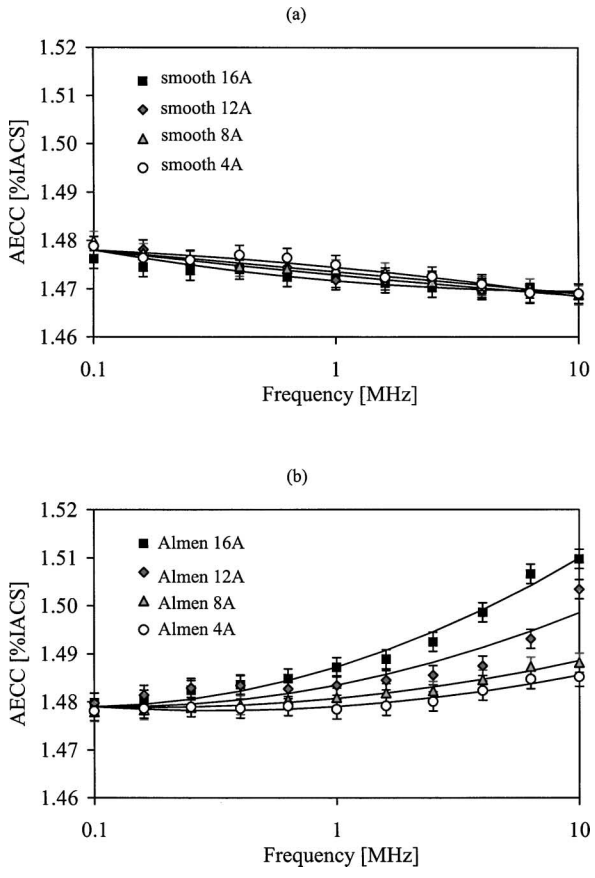

Fig. 11. Absolute AECC taken manually from the (a) smooth or unpeened and (b) shot-peened halves of the intact Waspaloy samples from 100 kHz to 10 MHz.

this discrepancy is not known, but we found that most of it is due to lift-off variations. During automatic scanning, additive errors due to inevitable lift-off variations are effectively rejected by measuring only the component normal to the lift-off direction in the complex impedance plane. However, multiplicative errors due to the decreasing sensitivity at increasing lift-off distances still could affect the data. We conducted an experiment to determine the effect of varying the lift-off, which was measured using a dial-gauge with approximately 2.5 μm accuracy, on the sensitivity of the AECC measurement. The results shown in Fig. 13 illustrate that for a 1.5-mm-diameter probe coil ±25-μm lift-off uncertainty results in a relatively small ±4% error at 100 kHz, but as much as ±15% error at 10 MHz, which could account for most of the differences we observed between manual versus automated testing, considering that there could have easily been ±25-μm lift-off uncertainty

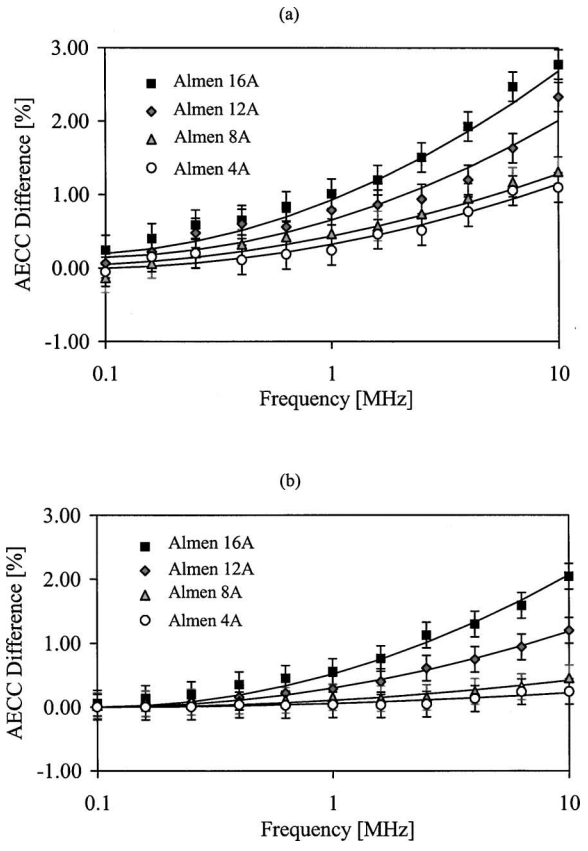

Fig. 12. Eddy current results after taking the difference in AECC between the peened and unpeened surfaces for (a) manual testing and (b) automated scanning.

in the AECC difference measurements during automatic scanning. Undoubtedly, this technical issue will have to be solved before the eddy current method becomes a reliable quantitative tool for residual stress assessment, but for the limited purposes of the present study we can conclude that the absolute and relative AECC measurements are at least consistent. Therefore the following extensive measurements on thermally relaxed specimens were all made by the much simpler relative technique using automatic scanning.

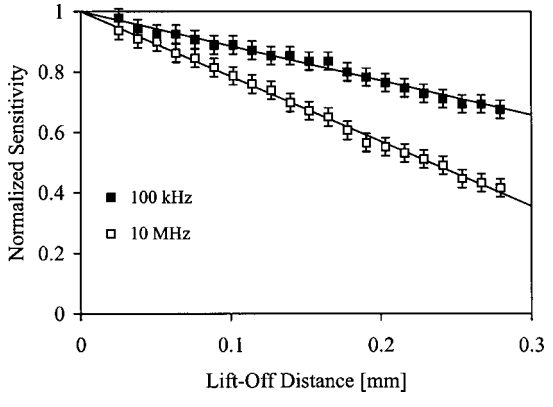

Fig. 13. A comparison of the effect of varying the lift-off at 100 kHz and 10 MHz on the normalized eddy current measurement sensitivity of a 1.5-mm-diameter probe coil.

5. MEASUREMENTS AFTER THERMAL RELAXATION

As previously mentioned, an essential feature of the sought measurement capability is that it must be capable of sensing changes in the residual stress profile after relaxation takes place in order to be useful for life prediction purposes. To determine if the eddy current approach meets this requirement, additional AECC measurements were conducted on shot-peened samples after different levels of thermal relaxation in order to verify the close correlation between the observed increase in the apparent eddy current conductivity at high frequencies and the retained residual stress.

The first question is whether the AECC difference between peened and unpeened surfaces diminishes with thermal relaxation or not. To answer this question, we inspected four shot-peened Waspaloy specimens of different peening intensity both before and after full thermal relaxation. Figure 14a shows the residual stress profiles as measured by XRD. An important byproduct of the XRD stress measurement is the cold work distribution over depth in terms of plastic strain as shown in Fig. 14b, which is based on the width of the particular diffraction peak of interest (the 311 peak was used for these Waspaloy measurements). We can conclude that the peening intensity has a relatively strong affect on the degree and depth of the resulting cold work in shot-peened samples, with the highest degree of plastic strain occurring just below the surface at each peening intensity. In addition to the XRD data obtained from intact specimens (solid symbols), Figs. 14a and 14b also show the corresponding data obtained after full relaxation for 24 hours at 900°C (empty symbols). It is evident that essentially complete stress relaxation occurred in the specimens. In comparison, roughly one-fifth of the original cold work effect, which can be fully eliminated only by actual recrystallization, survived below the surface. Figure 15 shows the AECC differences recorded on these intact and fully relaxed Waspaloy specimens. Within the uncertainty

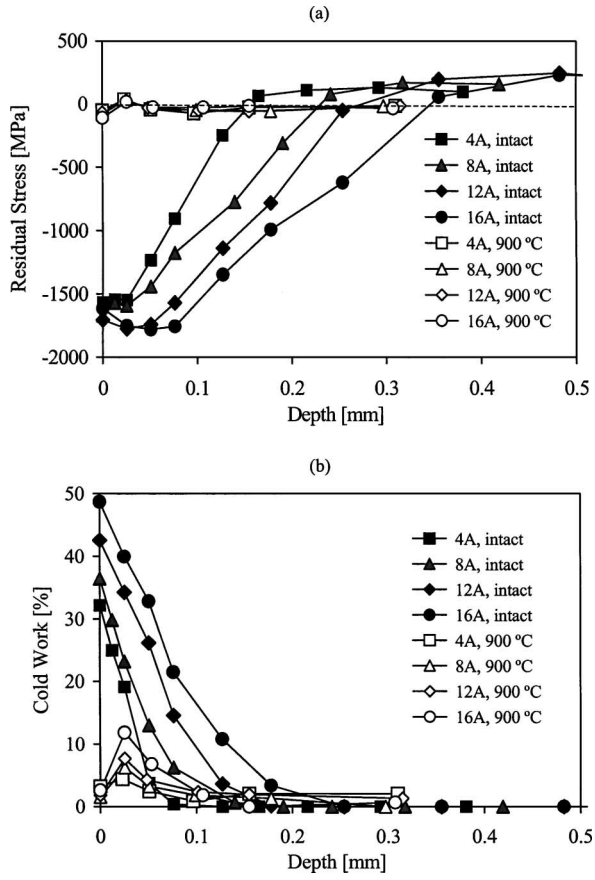

Fig. 14. X-ray diffraction (a) residual stress and (b) cold work profiles in a series of shot-peened Waspaloy samples before and after full relaxation (24 hours at 900°C).

of the eddy current measurement, the AECC difference completely vanished, which indicates that it is not only very sensitive to thermal relaxation, but also that it is mostly sensitive to the residual stress contribution since the cold work effect did not entirely disappear.

The next question is whether the AECC difference decays gradually with thermal relaxation or not, which is extremely important from the point of view of detecting partial relaxation. To answer this question, a Waspaloy specimen of Almen 8A peening intensity was gradually relaxed by repeated heat treatments of 24-hour each at increasing temperatures in 50°C steps from 300°C to 900°C in protective nitrogen environment. Figure 16 shows the decaying AECC difference between the peened and unpeened parts after each heat treatment. These results clearly indicate that the measured AECC difference gradually decreases during thermal relaxation and almost completely disappears after the 13th 24-hour heat treatment at 900°C, which is very promising for the possibility of sub-surface residual stress assessment in shot-peened Waspaloy.

The most crucial question is whether the AECC difference is proportional to the remaining residual stress throughout thermal relaxation or not. To answer this question, we subjected a couple of Waspaloy specimens of Almen 16A peening intensity to different thermal conditions, followed by eddy current conductivity and X-ray diffraction stress and cold work measurements. These samples were treated with three different thermal profiles at (i) 600°C for 24 hours, (ii) 600°C for 24 hours followed by 650°C for 24 hours, and (iii) 900°C for 24 hours and then compared to the original, as-received, shot peen condition. The XRD residual stress and cold work profiles for each case are shown in Fig. 17. There is a rather strong relaxation after the first heat treatment of 24 hours at 600°C, which is somewhat surprising as one would think that the shot peening induced residual stress would be more persistent in Waspaloy. However, we already found in the previous series of measurements on a Waspaloy specimen of Almen 8A peening intensity, which is supposed to be thermally more stable because of the lower level of cold work present in the specimen, that significant relaxation occurs at temperatures as low as 500°C (see Fig. 16), therefore these XRD results are not entirely unexpected. To the best of our knowledge, such early thermal relaxation in shot-peened Waspaloy has not been reported in the literature before and this phenomenon will have to be further investigated in the future. One possible explanation for this early relaxation is that these Waspaloy specimens were stress annealed prior to shot peening, which typically puts the material in its softest state. Another unexpected result is shown in the XRD cold work profiles where the degree of cold work is slightly higher in case (ii) than in case (i). This discrepancy is unusual, but the precise pedigree of the Waspaloy we used is unknown and samples may have come from plate stock with different rolling conditions.

For each case, eddy current conductivity measurements were performed between 100 kHz and 10 MHz. As before, differential measurements were made between peened and unpeened surfaces using automatic scanning. As shown in Fig. 18, the eddy current measurements are consistent with the XRD data in that the 600°C, 24-hour thermal treatment, i.e., case (i), caused a dramatic change in shot peen condition, as compared to the original. A comparison of the eddy current data for case (i) and case (ii) suggests

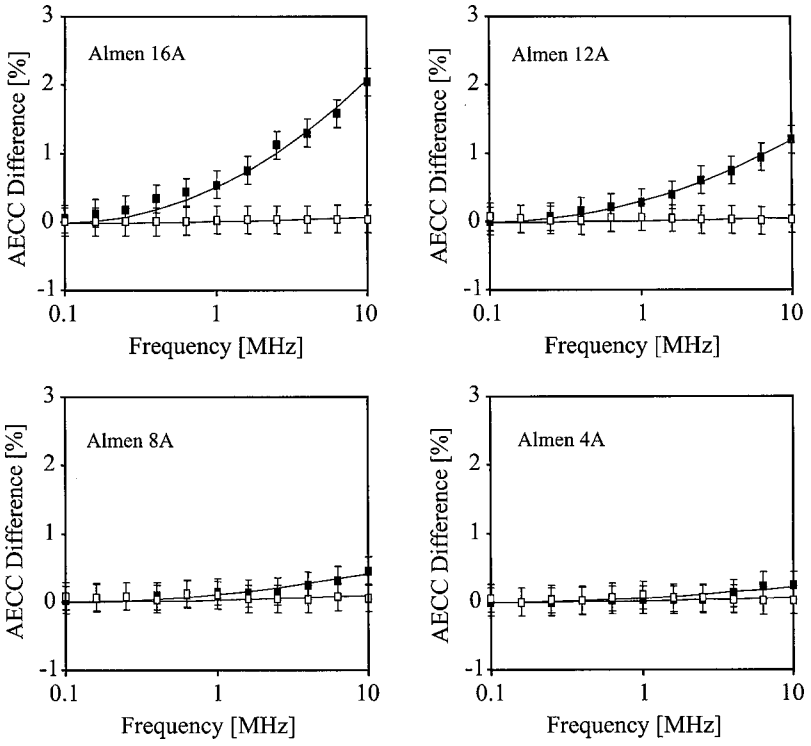

Fig. 15. AECC differences recorded on intact (solid symbols) and fully relaxed (empty symbols) Waspaloy specimens.

only a modest change in condition between the two, and case (iii) indicates virtually complete elimination of shot peen effects in the measured AECC. Overall, the decay of the AECC difference between the peened and unpeened specimens is roughly proportional to the decay of the sub-surface residual stress, although a more quantitative comparison has not been attempted yet. It should be mentioned that there are numerous analytical and numerical methods that could be exploited to invert the frequency-dependent AECC.[22–25] The conductivity profiles obtained from such inversion then could be used directly to assess the existing residual stress profile based on the empirically determined electro-elastic coefficient of the material. These efforts will be part of our follow-up study.

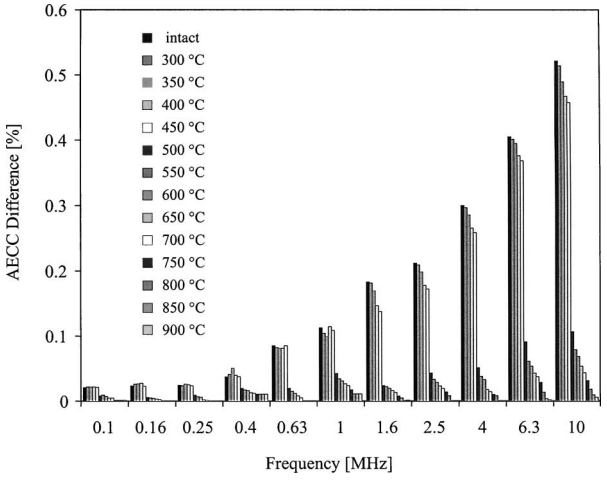

Fig. 16. The decay of AECC difference between the peened and unpeened parts of a Waspaloy specimen of Almen 8A peening intensity during gradual thermal relaxation.

6. CONCLUSIONS

Our experiments indicate that there exists a unique "window of opportunity" for eddy current NDE in nickel-base superalloys. At least six factors contribute to this fortunate constellation of material properties. First, the parallel stress coefficient of the electrical conductivity has a large negative value while the normal coefficient is smaller but also negative. As a result, the average stress coefficient is also large and negative, therefore the essentially isotropic compressive plane state of stress produced by most surface

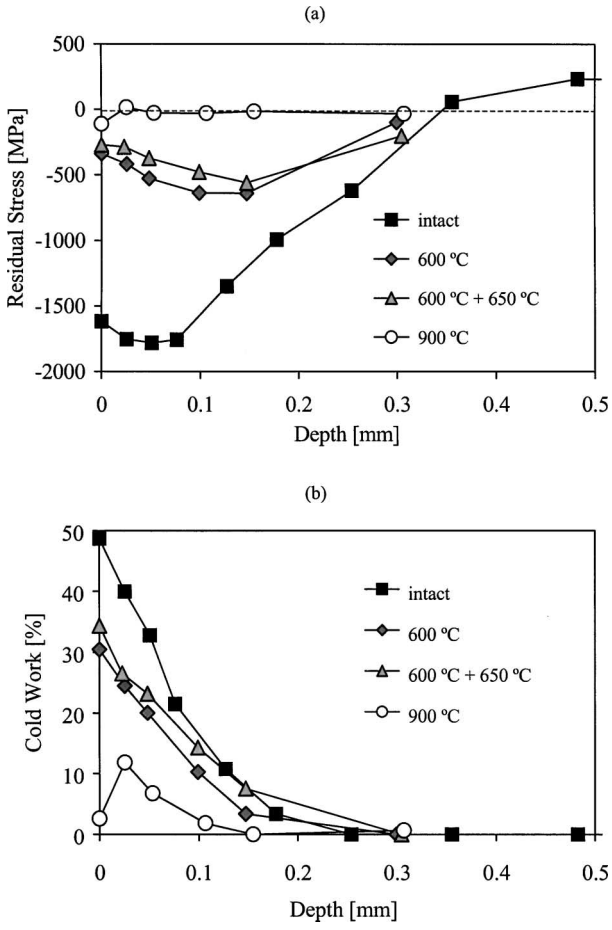

Fig. 17. X-ray diffraction (a) residual stress and (b) cold work profiles in a series of Waspaloy samples of Almen 16A peening intensity after different levels of thermal relaxation.

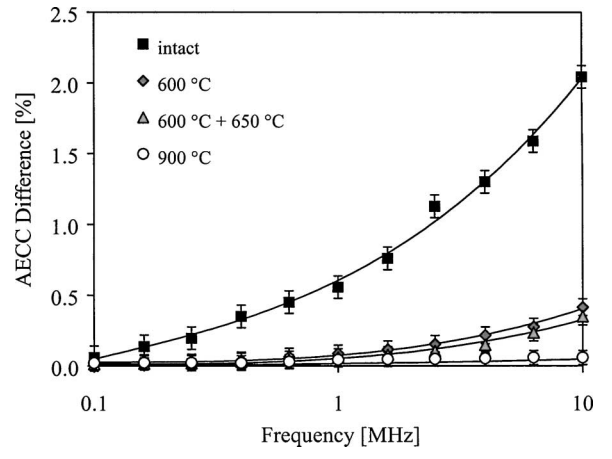

Fig. 18. Eddy current conductivity measurements in shot-peened Waspaloy of Almen 16A intensity (each heat treatment was 24 hours).

treatments causes a significant increase in the electrical conductivity parallel to the surface. Second, the electrical conductivity in nickel-base superalloys is rather low (≈1.5% IACS) therefore the penetration depth is relatively high at a given frequency (≈180 μm at 10 MHz). Therefore, at typical inspection frequencies we can detect the increasing conductivity due to the highly persistent residual stresses at larger depths that cannot be measured in a nondestructive way by X-ray diffraction, which is sensitive to the very unstable near-surface residual stresses only. Third, the hardness is relatively high therefore the spurious surface roughness is relatively small for typical Almen intensities (3A–8A) used on engine components, therefore the apparent conductivity drop due to this artifact is also relatively small. Fourth, for the same reason, the eddy current conductivity is not reduced significantly by increased dislocation density and other types of microstructural defects due to cold work, which cause the thermal instability of the near-surface residual stress in the first place. Fifth, these materials crystallize in cubic symmetry, therefore the electrical conductivity does not exhibit crystallographic anisotropy, and therefore the spurious crystallographic texture below the surface does not affect the measurement at all. Sixth, in spite of the very high nickel and iron content of these superalloys, neither the intact material nor the cold-worked surface layer exhibit perceivable magnetic permeability beyond slight paramagnetism, which otherwise could easily overshadow the much weaker electro-elastic effect due to piezoresistivity.

On intact shot-peened specimens we found that the excess AECC was proportional to the peening intensity. On partially relaxed shot-peened Waspaloy specimens we found that the measured AECC difference changed more or less proportionally to the remaining sub-surface residual stress. On fully relaxed Waspaloy specimens, the AECC completely vanished, which indicates that it is fairly selective to the residual stress contribution since the cold work effect did not entirely disappear. The close qualitative resemblance between the eddy current conductivity and XRD residual stress data leads us to believe that the eddy current approach has the potential to be exploited for nondestructive characterization of subsurface residual stresses in certain surface-enhanced nickel-base superalloys. The frequency-dependence of the excess apparent eddy current conductivity is consistent with the penetration depth of the compressive residual stress distribution and in a follow-up paper we will demonstrate that quantitative inversion of the stress profile from the conductivity spectrum is also

possible. However, it is obvious that further efforts are needed to fully realize the quantitative potential of the eddy current approach in terms of the exact weighting of the different effects, the material-dependent correlation to residual stress, and the rendering of residual stress profiles based on the measured frequency-dependent AECC.

ACKNOWLEDGMENTS

This work was partially supported by the Department of the Air Force under Contract No. F33615-03-2-5210. The authors would like to acknowledge valuable discussions with Waled Hassan of Honeywell Engines, Systems, and Services, Neil Goldfine and Vladimir Zilberstein of JENTEK Sensors Inc., and Norbert Meyendorf of the University of Dayton. The authors also wish to thank Curtis Fox, Brian Minda, Mike Perrino, and Mary Locke of the Department of Aerospace Engineering and Engineering Mechanics at the University of Cincinnati for their contributions to some of the eddy current measurements reported in this paper. The specimens used in this study were machined at Metcut Research, Inc., the shot peening was performed by Metal Improvement Co., and the X-ray diffraction measurements were done by Lambda Research.

REFERENCES

1. R. John, J. M. Larsen, D. J. Buchanan, and N. E. Ashbaugh, "Incorporating residual stresses in life prediction of turbine engine disks," Proceedings from *NATO RTO* (*AVT*) *Symposium on Monitoring and Management of Gas Turbine Fleets for Extended Life and Reduced Costs*, Manchester, UK, 8–11 Oct., 2001.
2. J. M. Larsen, B. Rasmussen, S. M. Russ, B. Sanbongi, J. Morgan, D. Shaw, J. Jira, D. Johnson, S. LeClaire, M. Blodgett, T. Moran, W. Stange, M. Meininger, and T. Fecke, "The engine rotor life extension (ERLE) initiative and its opportunities to increase life and reduce maintenance costs," *AeroMat Conference*, Long Beach, CA, June 12, 2001.
3. American Society for Metals, *Metals Handbook*, **Vol. 10**, *X-ray Diffraction Residual Stress Techniques* pp. 380–392, 1986, Metals Park, Ohio.
4. V. Hauk, *Structural and Residual Stress Analysis by Nondestructive Methods*, pp. 102–112, 1997, Elsevier, Amsterdam.
5. P. S. Prevéy, in *IITT International*, pp. 81–93, 1990, Gournay-Sur-Marne, France.
6. N. Goldfine, "Real-time, quantitative materials characterization using quasistatic spatial mode sensing," *41*st *Army Saganore Conference*, August, 1994.
7. N. Goldfine, D. Clark, and T. Lovett, "Materials characterization using model based meandering winding eddy current testing (MW-ET)," *EPRI Topical Workshop: Electromagnetic NDE Applications in the Electric Power Industry*, Charlotte, NC, August 21–23, 1995.
8. F. C. Schoenig, Jr., J. A. Soules, H. Chang, and J. J. DiCillo, "Eddy current measurement of residual stresses induced by shot peening in Titanium Ti-6Al-4V," *Mat. Eval.* **53**, pp. 22–26 (1995).
9. N. Goldfine and D. Clark, "Near surface material property profiling for determination of SCC susceptibility," *EPRI Balance-of Plant Heat Exchanger NDE Symposium*, Jackson, WY, June 10–12, 1996.
10. H. Chang, F. C. Schoenig, Jr., and J. A. Soules, "Eddy current offers a powerful tool for investigating residual strees and other metallurgical properties," *Mat. Eval.* **57**, pp. 1257–1260 (1999).
11. *A Primer on the Alternating Current Potential Difference Technique*, pp. 18–21, 1999, Matelect Systems, Nepean, Ontario.
12. A. I. Lavrentyev, P. A. Stucky, and W. A. Veronesi, in *Review of Progress in QNDE*, **Vol. 19**, pp. 1621–1628, 2000, AIP, Melville.
13. J. M. Fisher, N. Goldfine, and V. Zilberstein, "Cold work quality assessment and fatigue characterization using conformable MWM^{TM} eddy current sensors," *49*th *Defense Working Group on NDT*, October 31–November 2, 2000.
14. V. Zilberstein, Y. Sheiretov, A. Washabaugh, Y. Chen, and N. J. Goldfine, in *Review of Progress in QNDE*, **Vol. 20**, pp. 985–995, 2001, AIP, Melville.
15. P. M. Blodgett, C. V. Ukpabi, and P. B. Nagy, "Surface roughness influence on eddy current electrical conductivity measurement," *Mat. Eval.* **61**, pp. 765–772 (2003).
16. K. Kalyanasundaram and P. B. Nagy, "A simple numerical model for calculating the apparent loss of eddy current conductivity due to surface roughness," *NDT&E Intern.* **37**, pp. 47–56 (2004).
17. M. Blodgett and P. B. Nagy, "Anisotropic grain noise in eddy current inspection of noncubic polycrystalline metals," *Appl. Phys. Lett.* **72**, pp. 1045–1047 (1998).
18. M. Blodgett, W. Hassan, and P. B. Nagy, "Theoretical and experimental investigations of the lateral resolution of eddy current imaging," *Mat. Eval.* **58**, pp. 647–654 (2000).
19. P. W. Bridgman, The Physics of High Pressure, Ch. IX. *Electrical Resistance of Metals and Solids* pp. 257–294, 1970, Dover Publications, New York.
20. N. M. White and J. D. Turner, "Thick-film sensors: Past, present and future," *Meas. Sci. Technol.* **8**, p. 1–20 (1997).
21. S. U. Jen, T. C. Wu, and C. H. Liu, "Piezoresistance characteristics of some magnetic and non-magnetic metal films," *J. Magn. Magn. Mat.* **256**, pp. 54–62 (2003).
22. E. Uzal, J. C. Moulder, S. Mitra, and J. H. Rose, "Impedance of coils over layered metals with continuously variable conductivity and permeability—Theory and experiment," *J. Appl. Phys.* **74**, pp. 2076–2089 (1993).
23. S. J. Norton and J. R. Bowler, "Theory of eddy-current inversion," *J. Appl. Phys.* **74**, pp. 501–512 (1993).
24. E. Uzal, J. C. Moulder, and J. H. Rose, "Experimental-determination of the near-surface conductivity profiles of metals from electromagnetic induction (eddy-current) measurements," *Inverse Problems* **10**, pp. 753–764 (1994).
25. C. Glorieux, J. Moulder, J. Basart, and J. Thoen, "The determination of electrical conductivity profiles using neural network inversion of multi-frequency eddy-current data," *J. Phys. D: Appl. Phys.* **32**, pp. 616–622 (1999).